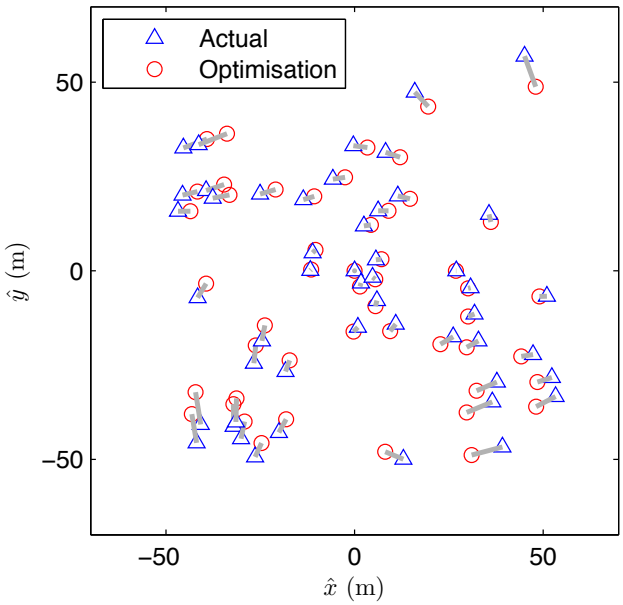

Figure 1: Example 1 - Synthetic relocation of 50 earthquakes in 2D using all constraints with noise $\bar{\sigma}_N = 0.02$. Actual and optimization event locations are identified by triangles and circles, respectively.

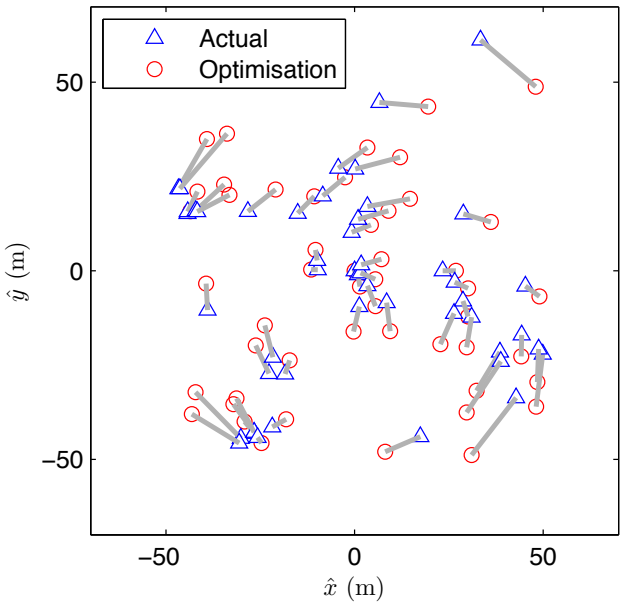

Figure 2: Example 2 - Synthetic relocation of 50 earthquakes in 2D using all constraints with noise $\bar{\sigma}_N = 2\epsilon(\delta_t)$. Actual and optimization event locations are identified by triangles and circles, respectively.

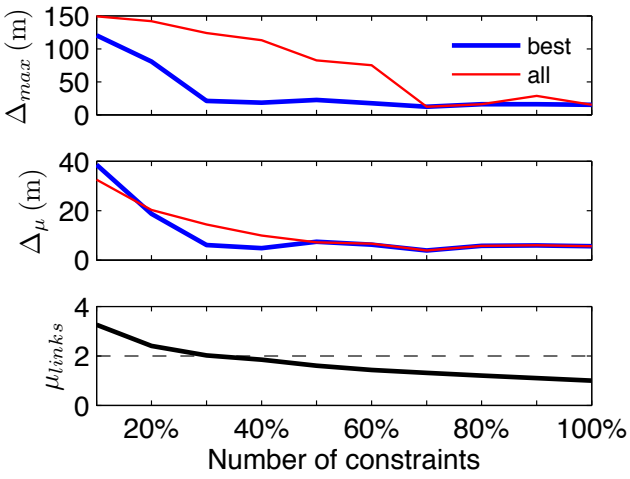

Figure 3: Example 3 - Statistical measures of error in the solutions for the 2D synthetic cases when all and best optimization results are considered. The statistics Δ_{max} and Δ_{μ} are the maximum and mean coordinate error, respectively. The bottom subplot shows the average minimum number of branches required to link the 2450 pairs.

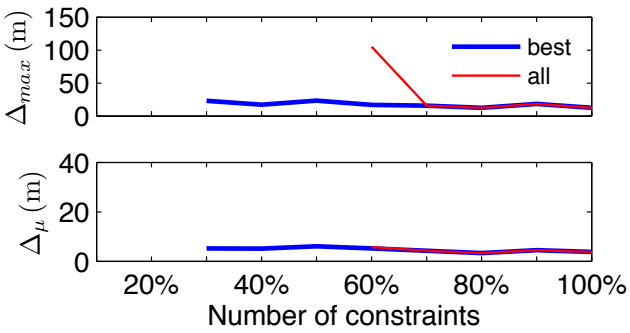

Figure 4: Example 4 - Statistical measures of error in the optimization solutions for the 3D synthetic cases when all and best results are considered. The statistics Δ_{max} and Δ_{μ} are the maximum and mean coordinate error, respectively. The absence of the lines below 60% and 30% indicates a breakdown in the solutions when all or best optimization result(s) are considered, respectively.

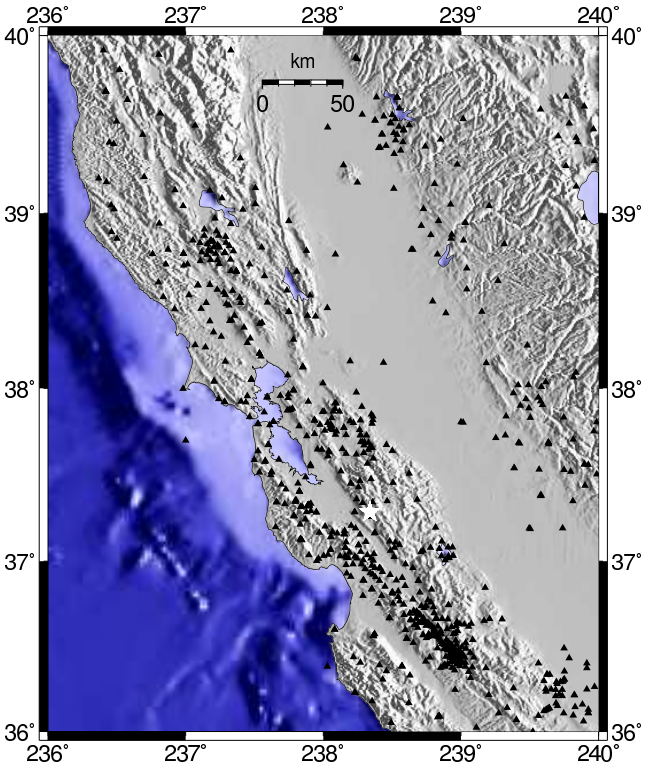

Figure 5: Map showing location of the Calaveras cluster (star) and 805 seismic stations (triangles).

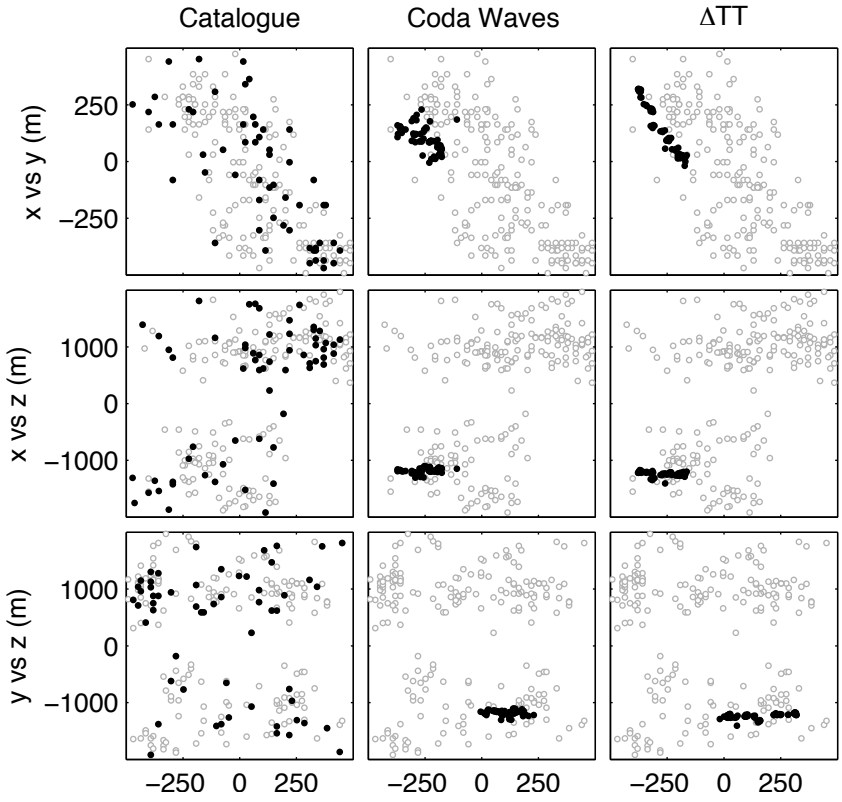

Figure 6: Example 5 - Comparison of relative earthquake locations using three different methods: catalogue location (column 1), CWI (column 2) and hypoDD (column 3). Note that in the case of the hypoDD and CWI inversions we consider only the 68 earthquakes in black, the gray catalogue locations for the remaining 240 (308-68) earthquakes are shown for the purpose of orientation only.

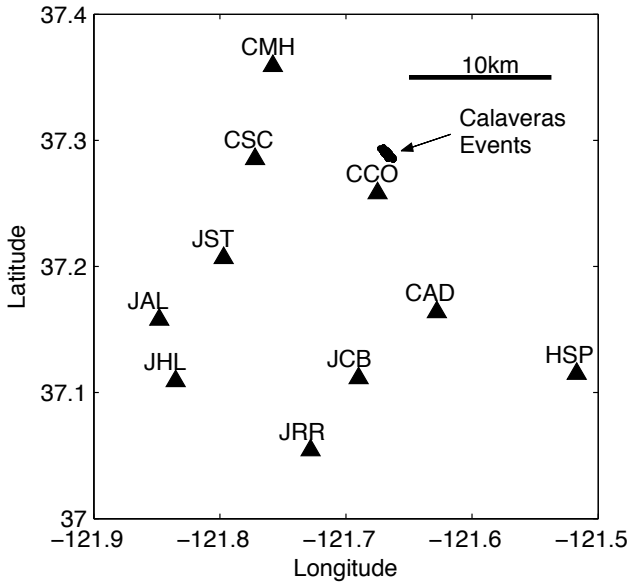

Figure 7: Location of the 10 stations (triangles) used to relocate the Calaveras events in Examples 6 to 8. Stations are removed one at a time according to the order in Table 3 and the events relocated. Events are indicated with circles.

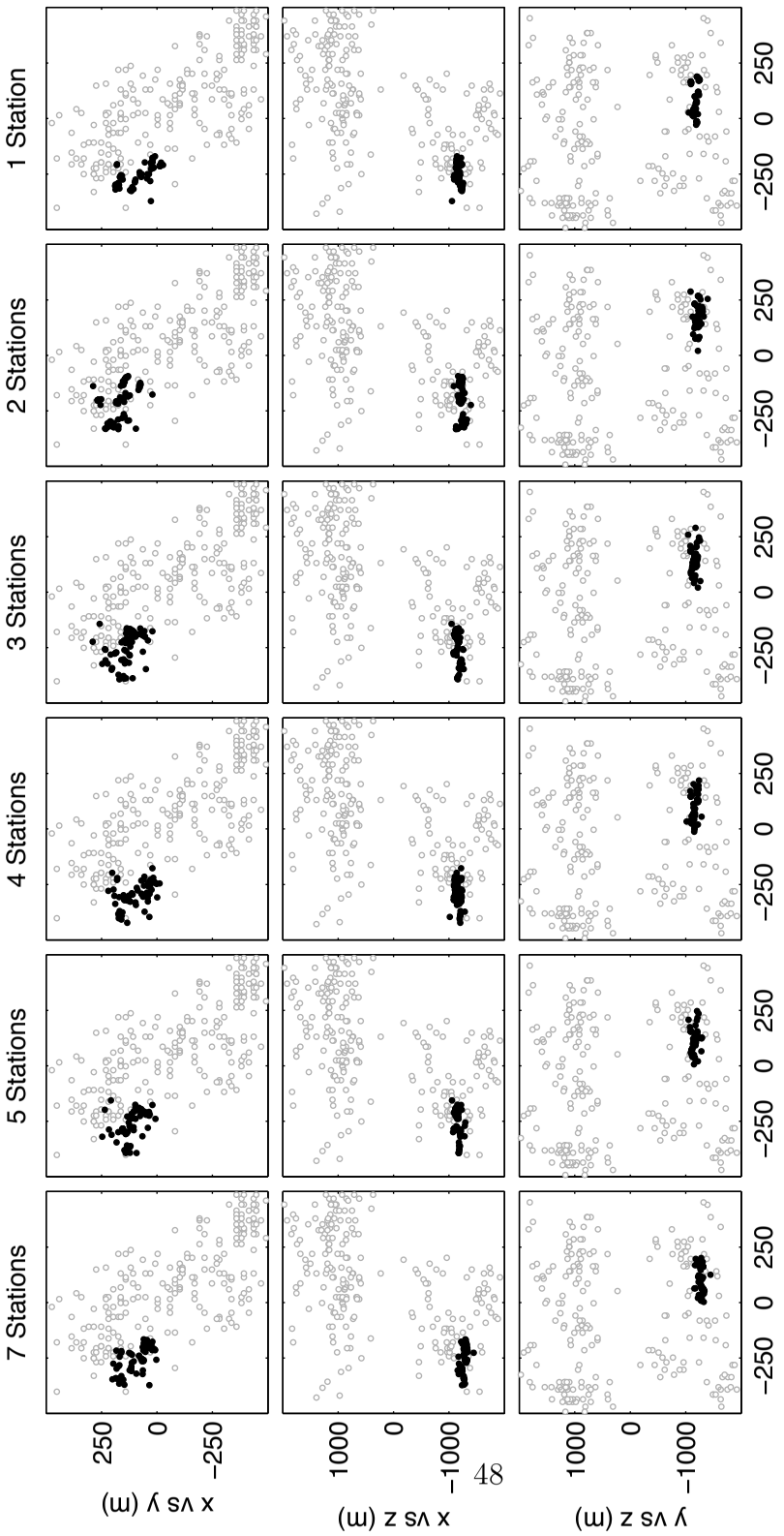

Figure 8: Example 6 - CWI relative locations with reduced stations.

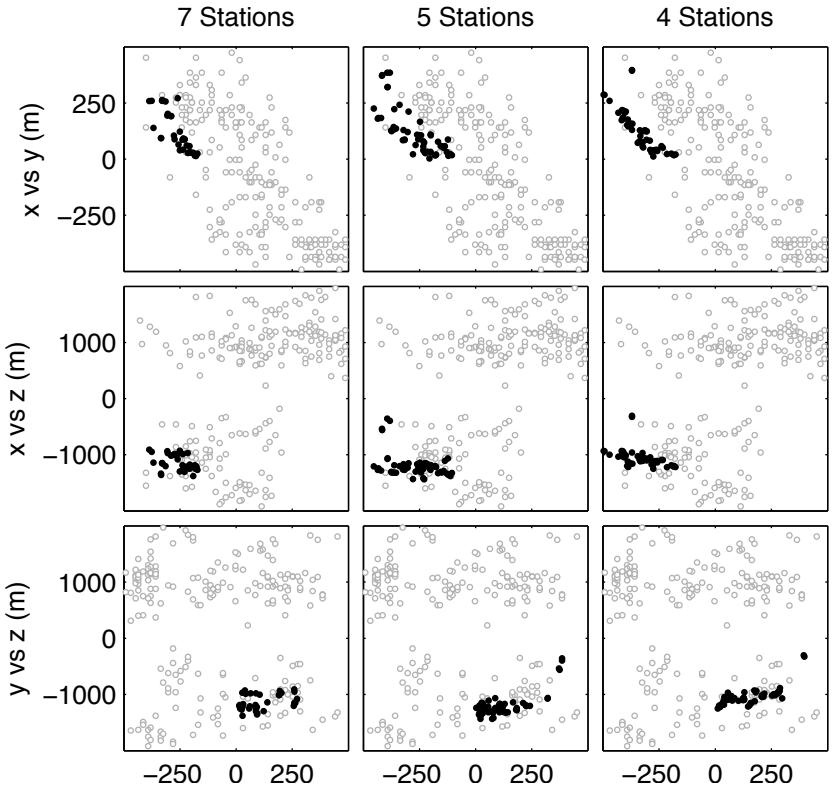

Figure 9: Example 6 - HypoDD (SVD) relative locations with reduced stations.

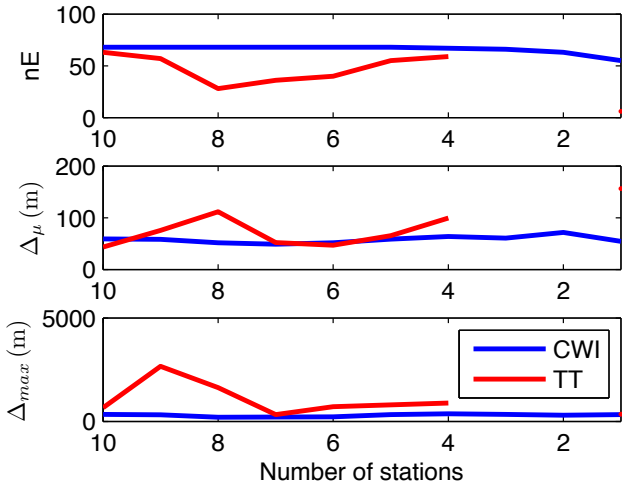

Figure 10: Example 6 - Number of constrainable events nE in the CWI and hypoDD inversions as a function of the stations considered (top). Mean (middle) and maximum (bottom) of the difference computed between the reduced station inversion results (CWI and hypoDD) and the complete hypoDD locations for all 308 events.

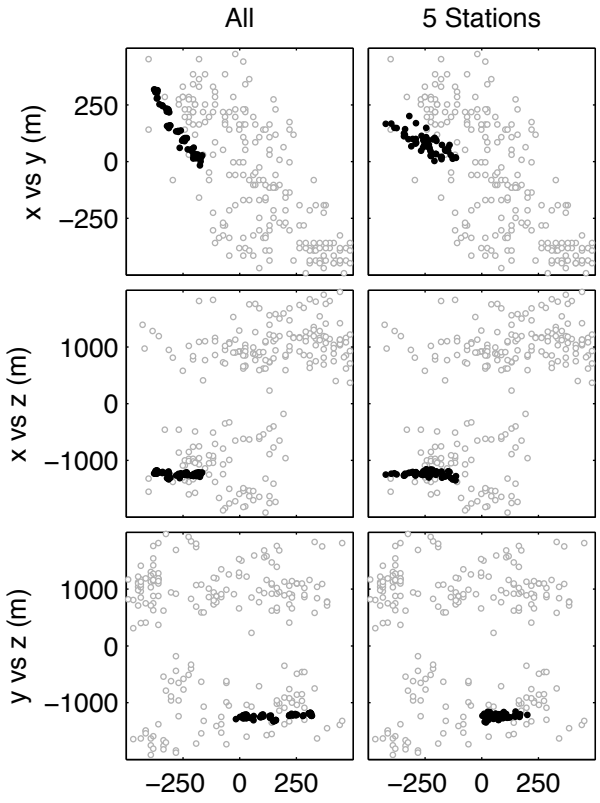

Figure 11: Example 7 - Combined HypoDD (SVD) and CWI relative locations using data form all stations (left) and 5 stations (right).

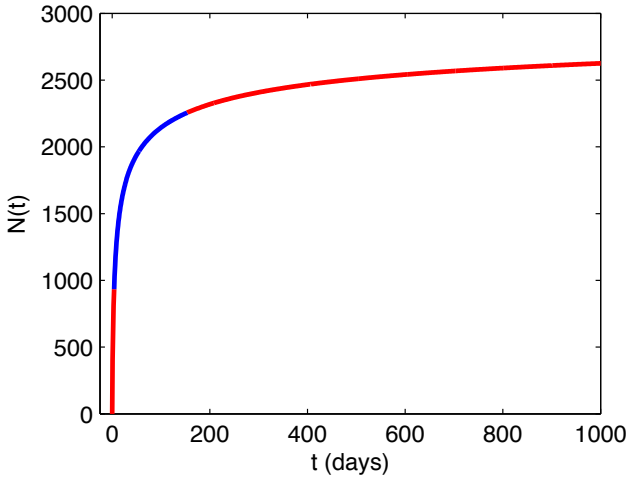

Figure 12: Cumulative number of aftershocks for the Hokkaido-Nansei-Oki, Japan $M_s = 7.8$ earthquake of 12 July 1993 using equation (33). The leftmost, middle and rightmost lines signify aftershocks occurring before, during and after the deployment of a pseudo temporary array installed 4 days after the main shock and left for 150 days. A temporary deployment of this kind will record roughly 50% of the aftershocks in the 1000 days following the mainshock.

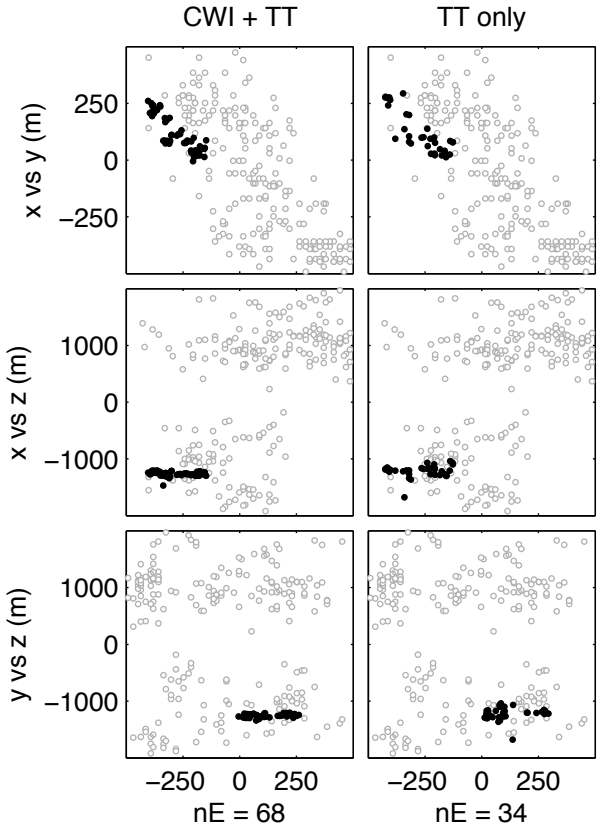

Figure 13: Example 8 - Mimicking the deployment of a temporary network by ignoring data from all but station CCO for 50% (or 34) of the events. Relative locations are shown for the combined CWI and travel time inversion (left) and the inversion with travel times only (right). Only by combining the data is it possible to locate all 68 events. Furthermore, combining the data leads to a solution more consistent with Figure 6.